City Research Online

City, University of London Institutional Repository

Permanent repository link: https://openaccess.city.ac.uk/id/eprint/23428/

Link to published version: http://dx.doi.org/10.1016/j.measurement.2019.107299

City Research Online: http://openaccess.city.ac.uk/   publications@city.ac.uk

Measurement and determination of encoder disc surface parameters in x-z planes using a conventional optical disc reading head

Lauryna Šiaudinytė [a,*], Vladas Juška [a,b], Vytautas Dumbrava [b], Darijus Pagodinas [b], Domantas Bručas [a],
Mindaugas Rybokas [a], Kenneth Thomas Victor Grattan [a,c], Boleslovas Krikštaponis [a]

[a] *Vilnius Gediminas Technical University, Institute of Geodesy, Sauletekio al. 12, LT-10223 Vilnius, Lithuania*
[b] *Kaunas University of Technology, Dept. of Electronics Engineering, K. Donelaicio g. 73, LT-44249 Vilnius, Lithuania*
[c] *City Graduate School, City University of London, Northampton Square, London EC1V0HB, United Kingdom*

ABSTRACT

Non-contact surface measurement methods as well as roughness parameter determination methods are analyzed in the paper. While most of the modern non-contact surface inspection methods require advanced instrumentation and a big budget, this study looks into a novel approach to non-contact encoder disc roughness measurements by using the proposed system attached to the rotary table with an implemented optical disc pick up head and the reference angle encoder. Application of a conventional optical disc laser reading system resulted in a cost effective and compact solution for a non-destructive angle encoder disc surface inspection. Assets and shortcomings as well as detailed analysis of the measurement procedure are explained in the paper. The experimental setup and the measurement results are presented within this article.

1. Introduction

The evaluation of surface roughness is a very important procedure in the field of optics and precision instrumentation, and is very valuable in other areas of engineering and medicine. Surface roughness is one of the main quality inspection features which are essential to know when the mechanical treatment of various components in industry or in the laboratory is performed [1–3]. A knowledge of surface parameters is relevant not only when the better operation of many automatic mechanical systems is considered, but also for a specific purpose such as using object surface scanning as a measurement technique.

All surface roughness measurement methods may be classified in two main groups – contact based and non-contact based methods. Sometimes the combination of both types is used for measurements [1,3]. One of the contact methods that has been regularly used for many years is the mechanical stylus method. However, it has a number of disadvantages such as limited lateral accuracy (which is restricted by the radius of the nib), typically exceeding 2–5 μm [4]. The other major disadvantage is that the mechanical

contact required may be a cause of a surface scratching and for valuable objects this is unacceptable. Further, this familiar method has low measurement speed and is difficult to automate. Achieving higher accuracy measurement with the contact method is limited by the noise generated by the measuring system. In spite of this, there are methods [5,6] which use generated noise to determine the roughness. Noise evaluation is thus important and often used in non-contact methods for surface measurement. This paper focuses on the non-contact optical methods in order to avoid many problems highlighted in the contact approach.

Optical methods are more often used due to their higher speed. The main optical methods are: profilometry, interferometry, atomic force microscopy, method of optical correlation, microwave [7] and laser speckle methods [5,8]. Some of optical methods are suitable for inspection of the smallest silicon components of micro-electro-mechanical systems [9]. White light optical interferometry [9,10] is often the key component in precision measurements due to its relatively small uncertainty and ease of use. These methods have long been reported as reliable, precise, fast and do not require any special preparation for the surface measurement to be made. However, the instrumentation itself often is expensive and this can be a drawback. The optical methods used together with the online measurement techniques are able to ensure roughness measurement in the range of 0.025–1.6 μm.

---

* Corresponding author.
E-mail address: lauryna.siaudinyte@vgtu.lt (L. Šiaudinytė).

Such methods are more stable in comparison to the contact-based stylus method and minimize the potential for damage [11]. The use of interference microscope for surface roughness measurements helps to increase the accuracy of up to 0.02 nm [12].

The former research revealed that CD and DVD pick up heads can be implemented in other measuring systems as a cost saving solution. Some approaches deal with the application fields such as accelerometry, profilometry and linear measurements [13–15]. Latest research suggests that CD and DVD pick up heads have a lot of potential for the instrumentation development in biochemistry and biosensing [16,17]. However, it was not applied for the determination of an angle encoder disc surface quality measurements.

The aim of this work is to develop and investigate an effective angle encoder disc surface roughness optical measurement method designed using a conventional optical disc laser reading head as one of its application fields. The method offers a number of advantages: a simplified structure, non-contact measurement principles and it is a low cost method since the optical head is widely used and commercially available. Further in this paper we present the design and main working principles of the proposed system followed by the experimental approach in which the surface roughness parameters and defects of the samples are determined. Results as well as their numerical characteristics are presented and analyzed throughout the paper. The generalization and summing up are presented in conclusions at the end of this article.

2. The design of the roughness measuring system

It is often needed to measure roughness of both large surface fragments and smaller segments simultaneously. Most of the evaluation methods used for surface quality monitoring do not allow the visualization of the measurement result in three-dimensional space. However, some of the methods, such as visual or contact methods do actually enable representation of such information in three-dimensional space. The use of a laser interferometer allows to measure the desired characteristics of the surface, but unfortunately the price of such instruments is significant, thereby limiting their use [10,18].

A novel rotary measuring system was designed in order to detect defects of the grating shape as well as to determine unevenness and roughness of the encoder disc and its coating. The grating shape defects can occur due to mechanical damage and dirt. Unevenness of coating thickness is especially relevant in high resolution discs because it creates a spatial distortion of a grating width and causes an error in angular position setting. The roughness of a grating surface diminishes the possibility of small defect detection.

There are alternative video methods which fully solve only the first task and are much more complicated in terms of hardware and software. It can be stated that the method being used in this research visualizes the disc surface in the X–Z planes. Y-coordinate is obtained by changing CD head position in radial direction.

Fig. 1 shows a theoretical representation of roughness and parameters R_a (arithmetic mean) and R_q (root mean square).

The main integral parameter R_a, the arithmetic average of the absolute values, is expressed in the following equation [19,20]:

$$R_a = \frac{1}{N} \sum_{i=1}^{N} |Z_i| \tag{1}$$

where N – number of realizations, Z_i - i-th measurement amplitude.

Another parameter, the mean square deviation value R_q, can be calculated using the classical equation:
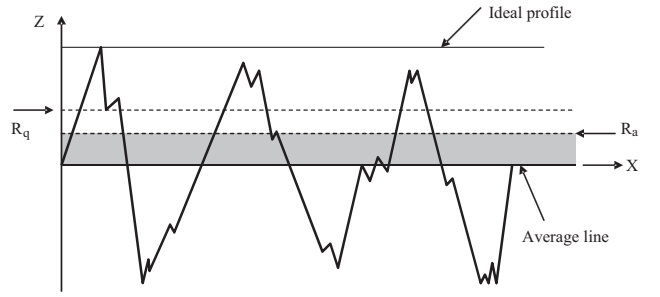

Fig. 1. Surface roughness parameters of the profile.

$$R_q = \sqrt{\frac{\sum_{i=1}^{N} (Z_i)^2}{N}} \tag{2}$$

Determination of these parameters enables us to evaluate the roughness of the metalized grating of the encoder disc.

2.1. Operating principle

During the measurements, the high frequency component could provide us with the information about surface's roughness, scratches or shape and contrast of the grating. Fig. 2 shows the structural scheme of a typical CD laser head unit. After crossing ¼ λ plate the beam was directed to the beam splitter and the measured surface, from which it reflected with a 180° polarization angle shift. Then the reflected beam passed through the cylindrical lens to the photodiode matrix (Fig. 2) [13].

In the setup, the laser beam was diffracted into 3 beams and collimated. The central beam had the highest intensity of 50% of light. Intensity of the side beams was 25%. The matrix consisted of 6 sectors of which 4 were used for the detection of the central beam and 2 for the detection of the side beams. The aperture of the reflected beam depends on the reflection point. Therefore, the purpose of the cylindrical lens was to change the aperture of the beams which pass to the detector. In case of the cylindrical lens absence, the aperture would always have the circular shape. Possible beam apertures and measurement signals are shown in Fig. 3.

Focused beam had a circular aperture as shown in Fig. 3b. When the beam is out of the focus, the aperture can change to Fig. 3(a and c). The operation points of focus error signal (FES) and correspond-
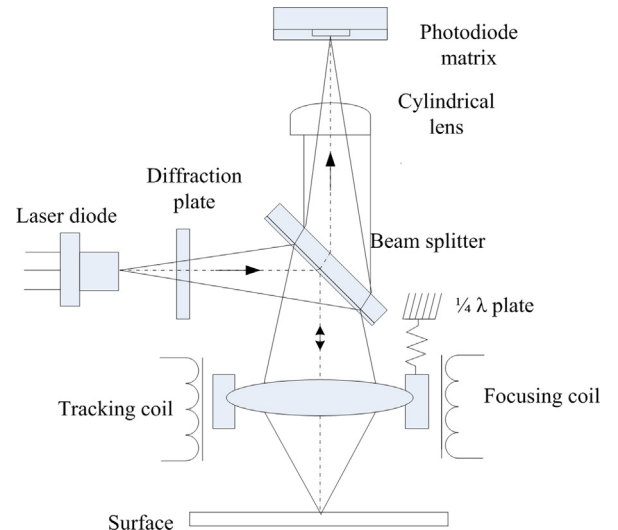

Fig. 2. The schematic view of the optical focusing system.

Fig. 3. Possible photodiode matrix aperture and measurement signals.

Fig. 4. Structure of the measuring system.

ing focusing apertures are shown in Fig. 3. Hence, beam aperture changes from different detection signals that are proportional to the distance from the focusing point. There are two types of signals which can be used for data evaluation: focus error signal (FES) and radio frequency (RF) signal data (Fig. 3e). Signals from photodiode matrix zone are formed according to (3) and (4) equations:

$$FES = (S_A + S_C) - (S_B + S_D) \tag{3}$$

where S_A, S_B, S_C, S_D – photodiode matrix zone signals.

RF signal is obtained according to Eq. (4):

$$RF = S_A + S_B + S_C + S_D \tag{4}$$

It is clear from Eq. (3) that if the laser beam is in focus, then the FES signal is equal to 0. RF signal data consists of the sum of photodiode matrix zone signals. In the structure of a typical system the FES signal with the small zone of the linear change was chosen (Fig. 3d). In this measurement system we have chosen the RF signal, which has significantly bigger amplitude and wider linear change zone with respect to FES signal case (Fig. 3e). Such means let us enhance the range of roughness measurement and increase the speed of the surface visualization. The experimental results are presented further in this paper.

The structure of the measurement system is shown in Fig. 4. The amplifier was connected to the conventional CD laser head (wavelength λ = 780 nm) unit. In this arrangement, the laser head signals were fed into the signal amplifier. These signals then became a subject of an additional signal processing and were forwarded to the Central Processing Unit (CPU), from which they reached the computer (PC) for display via an interface. The focus error signal (FES) used for forming and focusing with the coil control units was obtained from the amplified signal. The scanning component

used in the system had the electric gear unit replaced by a piezo-ceramic gear, in order to diminish the vibrations and reduce the error. This additional channel was narrowband (<300 Hz) and thus the surface roughness measurement signal had no influence on it. In addition, the PC was used to control a piezoelectric motor through the piezoelectric motor drive.

The amplified RF signal from the laser head output was sent to the measurement and control unit (MCU) for a further processing. The amplified RF signal was observed using a digital oscilloscope. MCU analyzes the signal obtained and detects the defects in a grating shape. This task was handled by a customized algorithm, which estimated 10 reference points throughout the grating period signal T, then compared them with the reference item and made a decision.

Surface scanning device was mounted on a precision rotary platform with a piezoelectric actuator and aerostatic suspension. These solutions resulted in a smooth rotation and low vibration level. The measurement distance was 1.5 mm. Angular position was monitored using an encoder RON 905, made by Dr. Johannes Heidenhain GmbH [21].

3. Experimental approach and the results

The experiment of this research provided us with an analysis of the results obtained using a low cost optical disc laser head as an approach to obtaining data of surface roughness and unevenness measurement. The main task of this work was to evaluate the roughness of the angle encoder disc surface and therefore, before testing the disc, the system was tested by using two ceramic reference plates with several surface fractions, typically of 0.3–6 μm each.

3.1. Calibration using reference plates and roughness calibration unit

Surface scanning has been performed using a precision rotary platform with a piezoelectric actuator and aerostatic suspension. The solutions resulting from such work have allowed a smooth rotation and low undesired vibration level in these measurements. Angular position was monitored using previously mentioned reference encoder [21].

Primary calibration of the measuring system was carried out in both static and dynamic modes. Two different calibration plates were attached to the rotary platform. Both of them with known thickness which differ from the reference plate by 8 ± 0.4 μm. Relative uncertainty of the calibration plate is 5%. Static calibration procedure is analogous to previously described and shown in Fig. 4. However, instead of the disc with the grating, the optical calibration plates were used for this part of the experiment.

The difference between obtained realization average values, divided by a known difference in thickness (8 μm), provided a value of the pursued static calibration coefficient (K_{st}) [mV/μm].

$$K_{st} = \frac{\bar{V}_1 - \bar{V}_2}{8} \qquad (5)$$

where $\bar{V}_1$ and $\bar{V}_2$ were arithmetic means of the calibration plate measurement results. For the experiment the broadband data channel was used. The signal was amplified and processed by a simple home-made circuit. In this case it was important to determine the calibration coefficients which described the sensitivity of the measuring system in order to transform the signal voltage fluctuations into the distance displacement.

Fig. 5 represents the results obtained from the measurements of two plates. The Y-axis shows the output signal voltage and the X axis represents the measurement points obtained using an oscilloscope Tektronix TDS3014B. The results have shown that there were overall 10 000 reference points. Looking at this closely, in the first plate, one scratch with a 9.2 μm depth is visible. An average of the difference in thickness gives the calibration coefficient, K_{st} = 40.9 mV/μm.

The level of rapid fluctuations (the total noise), was measured during a movement and is 0.0067 μm, illustrating the surface roughness. The internal noise level of the measuring system was determined to be 0.0084 mV. This means that the measurement of features seen in the sample are almost four times larger than the base signal level due to the noise.

High frequency component is proportional to the roughness of the plate and the noise level. It can be determined effectively through Allan variance [22] calculation:

$$D_a = \frac{1}{N-1} \sum_{i=1}^{N} (V_i - V_{i-1})^2 \qquad (6)$$

where D_a – high frequency component; N – number of measurements; V_i – i-th measurement value, respectively a total value of the rapid fluctuation signal. When the platform is rotating, the resulting dispersion of rapid fluctuations σ_{rms}^r and noise σ_{rms}^n can be calculated as follows:

$$\sigma_{rms}^{r+n} = \sqrt{D_a} \qquad (7)$$

Usually, after Allan filtration, the plate unevenness component σ_{rms}^t is found. Transfer function module of the filter is:

$$|H_A(jf)|^2 = \frac{2\sin^4(\pi Tf)}{(\pi Tf)^2} \qquad (8)$$
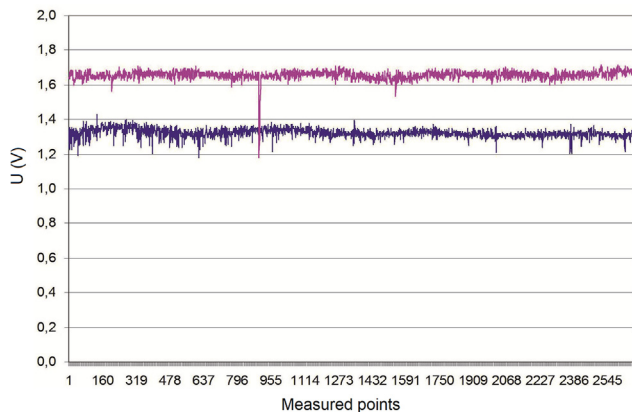
where f – signal frequency, T – period of measurement. When T is changing, it is possible to alter the range of the recorded fluctuations.

After stopping the platform rotation, the noise component σ_{rms}^n was measured. Table 1 shows the static calibration results of the measuring system.

During the signal processing (filtering) the random components σ_{rms}^r, σ_{rms}^n are significantly suppressed, and the influence of the unevenness depends on the ratio of spatial wavelength of the unevenness λ_t and the length l_{pl}. In the worst case, when the ratio is $\frac{\lambda_t}{l_{pl}} = 2$, the half wavelength fits in the whole length of the plate. Then the random error component caused by the unevenness reaches its highest value with the amplitude $\Delta Z_m = 3\sigma_{rms}^t$. The calibration error in this case was $0,7\Delta Z_m$, and the value of $\pm 3\sigma$ was equal to ±45 μm.

In order to determine the dynamic calibration coefficient, a surface roughness standard plate OPTC50496 was chosen together with a portable surface roughness instrument TR200. Fig. 6 generated by the oscilloscope, shows the obtained signal of the standard roughness plate. The segments of the beginning and the end of the plate as well as surface roughness areas are clearly visible in Fig. 6 together with the information about the duration of measurement and the voltage.

Table 2 shows the measurement results obtained from the statistical summary of the dynamic treatment carried out as an outcome of several successful implementations of a series of measurements.

As R_{aREF} (average roughness amplitude of the reference plate) is 1.6 μm, the value of the dynamic calibration coefficient can be found as a ratio of average roughness amplitudes of the measured surface and the reference plate. Since the average roughness amplitude of the measured plate is R_{aMEAS} = 0.041 μm, the dynamic calibration coefficient was determined K_{dyn} = 25.6 mV/μm.

As well as static calibration coefficient, dynamic calibration coefficient depends on how enhanced the treatment process is. Therefore, they are effective just for a certain realization of the measurement device.

3.2. Experimental results of the angle encoder disc calibration

The effect of noise in surface roughness measurement is discussed in publications [6,23]. It is obvious that the result of the averaging process is to mask the scratches, while the disparities of the surface can be easily evaluated from the slower changing view of the result. The distance between these features can easily be calculated knowing the number of pixels between them and the length of the section overall. In this case, it is four micrometers for one reference point where this parameter depends on the speed of rotation of the platform. If it reduces, it is possible to obtain a higher resolution in the measurement, which limits the minimum threshold value of the rotation speed. Any rotation speed imbalance can distort the scale and such an imbalance grows significantly when the platform rotation speed is reduced. Therefore, a compromise between a resolution and scale nonlinearity was sought and used in this work. In Fig. 7, surface measurement results of a rotary encoder disc are presented.

Fig. 5. Calibration using the reference plates.

Table 1
Static calibration results.

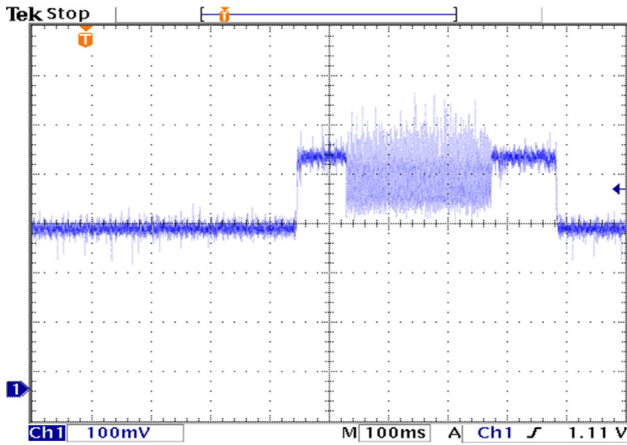| Static calibration coefficient, K_{st}	Noise σ_{rms}^n	Fluctuations σ_{rms}^r	Unevenness σ_{rms}^t
40,9	0.19	0.24	0.22

Fig. 6. Signal of the standard roughness plate.

Table 2
Statistical results of measurement.

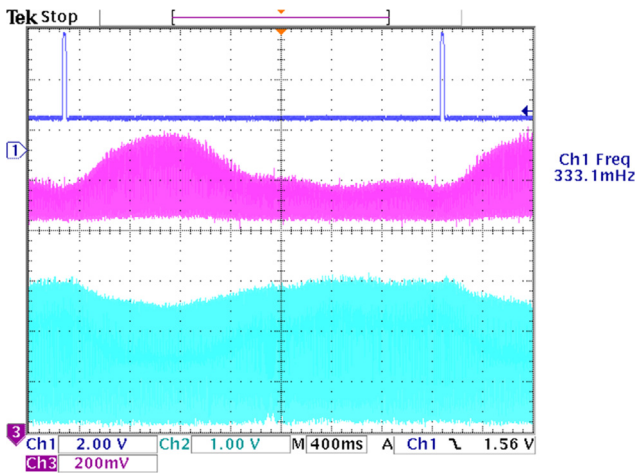| Realization	Average, V	Average roughness amplitude R_a, μm	Roughness amplitude R_q, μm
1	1.178	0.041	0.049
2	1.180	0.041	0.051
3	1.179	0.040	0.050

Fig. 7. Disc grating surface measurement.

The disc grating is visible in Channel 1 diagram of Fig. 7. Channel 2 and Channel 3 of Fig. 7 show the traces of the envelope of the disc which represent the thickness of the disparities.

Fig. 8 shows a real signal of the grating with some defects. The first defect clearly indicates the mechanical damage to the grating line (point 163), therefore, this disc must be discarded, the second damage at point 175 indication can be caused by dirty surface.

A customized software was created for the automated detection and classification of the grating defects. As a reference, for the angular position determination, the signal of Heidenhain RON 905 encoder was used (Fig. 9).

In this case, the signal of the reference encoder is used to analyze the grating of the encoder disc under test as well as to determine the dynamic parameters of the rotary platform. Fig. 10 shows a piezoceramic actuator control signal. It is obvious that the beginning of the movement (the signal of the reference encoder) is
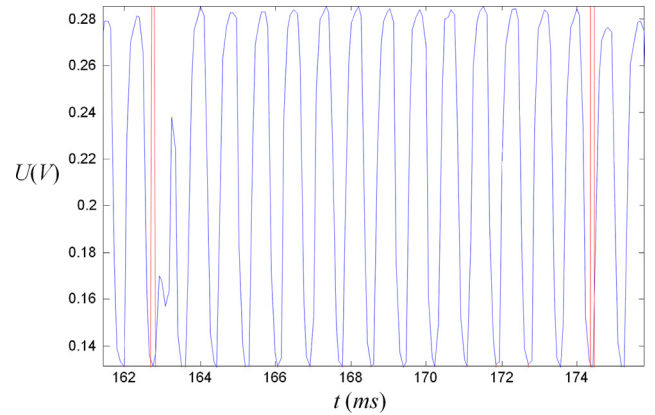
Fig. 8. Signal of the disc grating with defects.
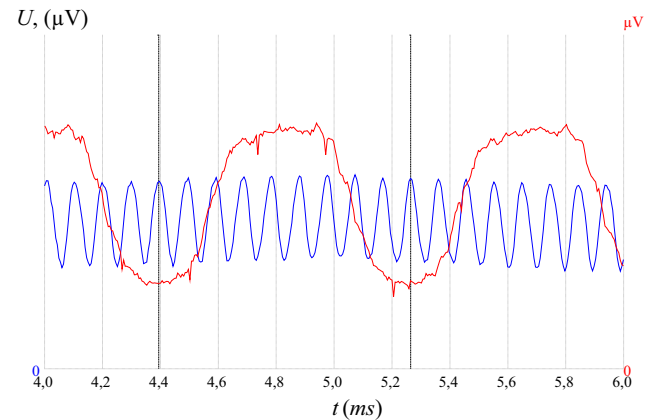
Fig. 9. The signals of both the reference encoder and the disc under test (lower frequency).
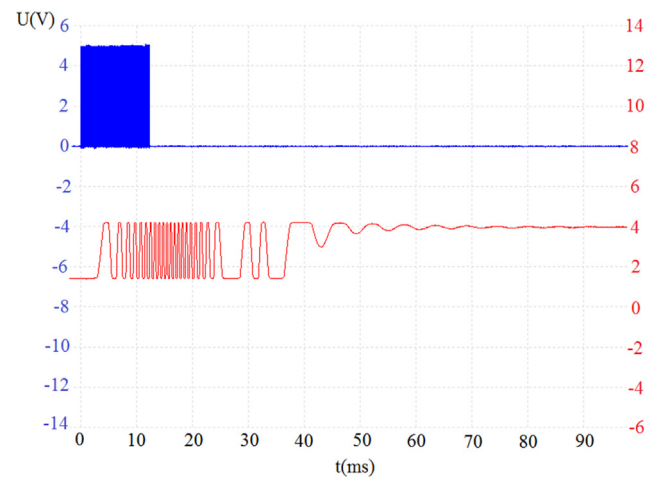
Fig. 10. Piezoceramic actuator control signal.

delayed due to the rotary platform inertia during switching on and off.

Usually the surface roughness is estimated using an integral parameter R_a. However, by using the system described in this paper, it is possible to perform the surface profile evaluation, which gives more information about the measured surface. A disc surface profile with a mechanical damage has been chosen to carry out the experiment.

The surface defect depth exceeded measuring range of the device (20 μm (K_{st} = 49[mV/μm]) as shown in Fig. 11. Scratch width can be found easily because we know the angular frequency ω and rotation radius R.

Profile determination is very important for the surface coating structure analysis and arrangement of different fraction particles. A typical example for this is the moisture-repellent coating. The results for the glass plate coated with a moisture repellent nano-material grating are shown in Fig. 12. It is evident that the resulting curve consists of both rapidly changing components and slow fluctuations.

Slow fluctuations can indicate that the entire plate pattern has some integral irregularities. The rapidly changing parameters are better seen within a range of 100 μm as shown in Fig. 13 where the shown instantaneous roughness peaks are up to 3 μm.

The results demonstrate that the proposed laser surface roughness measurement method enables an effective measurement to be made even within the range 0.5–1.0 μm. By knowing these parameters, it is easier to control the consistency of the coating of materials during the manufacturing process. The surface roughness directly depends on the characteristics of these composite materials and the proportions of their composition.

Fig. 14a) shows the actual experimental arrangement designed according to the schematic view showed in Fig. 4. The surface scanning device includes precision rotary platform with a piezoelectric actuator and aerostatic suspension [24,16]. A laser scanning head,
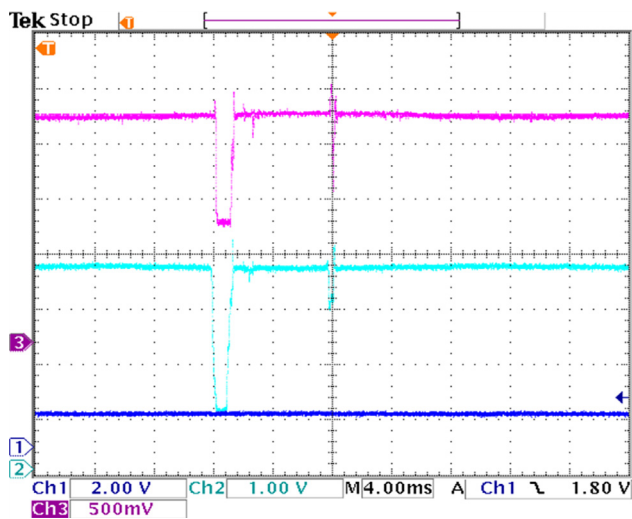

Fig. 13. The results of the adhesive surface roughness measurement.

Fig.14. Surface laser scanning device.

Fig. 11. Disc surface profile with segments of mechanical damage.

Fig. 12. The results of the adhesive surface roughness measurement.
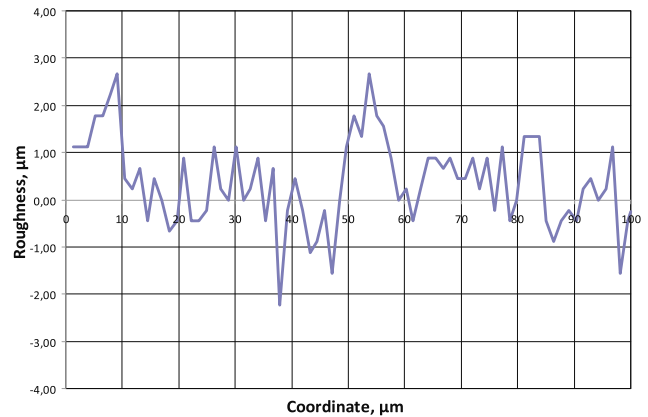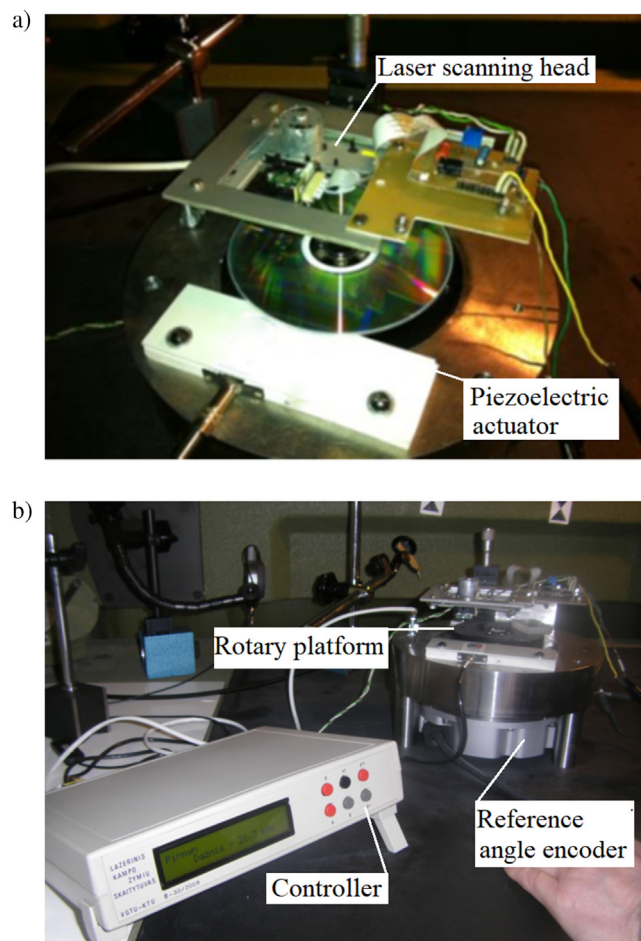
primary photoreceiver and signal amplifiers were placed on the top of the rotary platform. Fig. 14b) shows an overview of the complete measurement unit.

4. Conclusions

The research undertaken has revealed that it is possible to perform an effective surface roughness evaluation, with a good repeatability, using the optical disc laser reading head. The advantage of such a device is that it can be used during the angle encoder

disc manufacturing process not only for surface quality control but also, in combination with high-precision algorithms, similar as described in [25] for the determination of the angular position of the encoder grating. Furthermore, it can be used for the surface parameter and imperfection analysis of other textured objects, as the approach offers a rapid, often preliminary evaluation when this is required. At the same time the laser measuring system might also be used for surface coating structure analysis which is hardly possible to achieve by using other instrumentation. To demonstrate the efficacy of the device, a calibration procedure has been described and the results of roughness measurements using the proposed setup are presented in paper. Using proposed approach the surface roughness can be measured within the range of 0.5–20 μm. Since the device does not need a low speed focusing channel FES, the relatively high surface visualization speed can be achieved and the surface parameter measurement range can be increased. Moreover, the level of parasitic vibrations is low because of the piezoceramic drive used for the system rotation. One of the main advantages of the proposed setup is that the roughness of the surface and the angular position of the disc grating can be measured simultaneously because of the reference angle encoder implemented into the measuring system.

Declaration of Competing Interest

The authors declare that they have no known competing financial interests or personal relationships that could have appeared to influence the work reported in this paper.

Acknowledgement

References

[1] Y. Shen, Y. Wang, J. Zaklit, Development of an optical surface characterization sensor for simultaneously measuring both 3-D surface texture and mechanical properties, IEEE Conf., Sens. (2010) 1892–1895.

[2] T. Yang, W. Xue, Y. Liu, Influence of machining methods on wood surface roughness and adhesion strength, in: Proc of International Conference on Biobase Material Science and Engineering (BMSE), 2012, pp. 284–287.

[3] J. Zaklit, Y. Wang, Y. Shen, N. Xi, Quantitatively characterizing automotive interior surfaces using an Optical TIR-based texture sensor, in: Proc. of IEEE International Conference on Robotics and Biomimetics (ROBIO), 2009, pp. 1721–1726.

[4] X.M. Xu, H. Hu, Development of non-contact surface measurement in last decades, Proc. Intern. Conf. Measur. Technol. Mechatron. Autom. (2009) 210–213.

[5] X. Chen, Z. Liu, Z. Zhang, The measurement of planning surface roughness by neural networks based on image, in: Proc. of IEEE Sixth International Conference on Natural Computation (ICNC), 2010, pp. 705–708.

[6] S.Z. Sahwi, A.M. Mekawi, Effect of noise on surface roughness measurements, in: Proc. IEEE Instrumentation and Measurement Technology Conference, Brussels, Belgium, 1996, pp. 232–235.

[7] S.E. Park, L.F. Famil, S. Allain, E. Pottier, Surface roughness and microwave surface scattering of high-resolution imaging radar, IEEE Geosci. Remote Sens. Lett. (2014) 756–760.

[8] M. Hassan, B. Gaitan, I. Ilev, Decontamination of medical device surface using ultrashort pulsed laser irradiation, in: Conference on Lasers and Electro-Optics (CLEO), 2014, pp. 1–2.

[9] J. Krauter, M. Gronle, W. Osten, Optical inspection of hidden MEMS structures, Proc.of SPIE Optical Metrology, Optical Measurement Systems for Industrial Inspection, 2017.

[10] P. Groot, Design of error-compensating algorithms for sinusoidal phase shifting interferometry, Appl. Opt. 48 (35) (2009) 6788–6796, https://doi.org/10.1364/AO.48.006788.

[11] Y. Dong, An overview of optical methods for in process and on-line measurement of surface roughness, Proc. IEEE Int. Conf. Comput. Mechatron. Control Electron. Eng. (CMCE) (2010) 35–37.

[12] C. Saxer, K. Freischlad, Interference microscope for sub-Angstrom surface roughness measurements, Proc. Conf. Opt. Measur. Syst. Ind. Inspect. (2003) 37–45.

[13] J.W. Chieh, S.K. Hung, Transforming a CD/DVD pick-up-head into an accelerometer, in: Proc. of 2009 IEEE/ASME International Conference on Advanced Intelligent Mechatronics, 2009, pp. 493–497.

[14] G. Gerstorfer, B.G. Zagar, Development of a low-cost measurement system for cutting edge profile detection, Proc. of IMEKO TC2 Symposium Hangzhou, China, 2010.

[15] A. Makdissi, F. Vernotte, E. De Clercq, Stability variances: a filter approach, IEEE Trans. Ultrason. Ferroelectron. Freq. Control 57 (2010) 1011–1028.

[16] E.T. Hwu, A. Boisen, Hacking CD/DVD/Blu-ray for biosensing, ACS Sensors 3 (2018) 1222–1232.

[17] M. Shi, S.H. Weng, X. Li, H.Z. Yu, Digitized molecular detection on off-the-shelf Blu-ray discs: Upgraded resolution and enhanced sensitivity, Sens. Actuators, B: Chem. 242 (2017) 79–86.

[18] T.V. Vorburger, H.G. Rhee, T.B. Renegar, Jun-Feng (John) Song, A. (Alan) Xiaoyu Zheng, Comparison of optical and stylus methods for measurement of rough surfaces, Int. J. Adv. Manuf. Technol. 33 (2007) 110–118.

[19] A. Pino, J. Pladellorens, O. Cusola, J. Caum, Roughness measurement of paper using speckle, Opt. Eng. 50 (9) (2011).

[20] Standard ISO 4287. Geometrical Product Specifications (GPS)-Surface texture: Profile method -Terms, definitions and surface texture parameters, 1997.

[21] V. Giniotis, V. Grattan, M. Rybokas, D. Brucas, Analysis of measurement system as the mechatronics system, in: Proc. 13-th IMEKO TC1-TC7 Joint Symposium, 13-th Journal of Physics: Conference Series, 2010, pp. 1–6.

[22] I. Nashtara, R. Parkin, M. Jackson, P. Mueller, A novel surface profile measurement system, AU J. Technol. 10 (3) (2007) 203–209.

[23] T. Jeyapoovan, M. Murugan, B. Clemend Bovas, Statistical analysis of surface roughness measurements using laser speckle images, Proc. IEEE Word Congr. Inf. Commun. Technol. (2012) 378–382.

[24] D. Brucas, V. Giniotis, Measurement of angular displacement by means of laser scanner, J. Vibroeng. 12 (2010) 177–184.

[25] P. Yuan, D. Huang, Z. Lei, C. Xu, An anti-spot, high-precision subdivision algorithm for linear CCD based single-track absolute encoder, Measurement 137 (2019) 143–154.